

# Radiation from a Ferrite Filled Parallel Plate Waveguide with a Finite Periodic Slot Array in the Upper Plate

Kazuo Nishimura

Faculty of Science and Technology, Ryukoku University

1-5, Yokotani, Seta-oecho, Otsu, Shiga, 520-2194 Japan, Email: nisimura@rins.ryukoku.ac.jp

## Abstract

This paper presents radiation characteristics of a finite periodic slot array in a parallel plate waveguide filled with a transversely magnetized ferrite. The characteristics are analyzed by using the moment method and estimated numerically under the condition that the fundamental  $TE_1$  mode is only the propagating mode in the unperturbed parallel plate waveguide. It is theoretically explained how the characteristics can be tuned and the radiation patterns can be controlled by varying the dc magnetic field applied to the ferrite.

## 1. INTRODUCTION

Recently, research on RF electronic controllable high frequency devices and circuits has been paid attention to [1]. Research on microwave ferrite devices is a kind of the research on the RF controllable electronic high frequency devices. Until now, the vigorous development and research on the microwave ferrite devices such as isolators, circulators, phase shifter, delay lines, magnetically tunable resonators has been carried out by using anisotropy and frequency dependence of the permeability of ferrite that can easily be controlled by an external dc magnetic field [2]-[4]. On the other hand, research on antenna applications of ferrite materials has not been carried out extensively.

As research on antenna applications using ferrites, electronic scanning of the radiation pattern of an open-ended rectangular waveguide filled with ferrite [5],[6], electronic scanning of an antenna loaded with circularly arrayed ferrite bars [7], electronic scan of a millimeter-wave leaky wave antenna with a periodic structure loaded with ferrite [8]-[11], and microstrip antennas on a ferrite substrate [12]-[18] have been researched. Of these, the periodic ferrite structure can work not only as a leaky-wave antenna but also as a magnetically tunable Bragg reflection filter. So, research on propagation in the periodic ferrite structure is very interesting. The Bragg reflection characteristics and leaky-wave antenna characteristics of the infinite periodic ferrite structures have been characterized theoretically by means of the improved perturbation method [8], the singular perturbation method [11], and spectral domain method [19], [20]. As long as the author knows, the analytical research on ferrite waveguides with a finite periodic structure

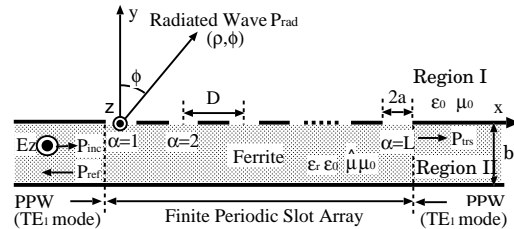


Fig. 1: A finite periodic slot array in a parallel plate waveguide filled with a transversely magnetized ferrite.

has been carried out little. So, the author have theoretically explained the radiation characteristics of a slotted parallel plate waveguide filled with a transversely magnetized ferrite by means of the method of moments. Then, the author have discussed the magnetic tunability of the radiation frequency band of the slotted parallel plate waveguide filled with ferrite and radiation pattern control by an applied dc magnetic field [21].

In this paper, radiation characteristics of a finite periodic slot array installed in an upper plate of a parallel plate waveguide filled with a transversely magnetized ferrite are analyzed by means of the method of the moments [21]-[24] in the case which only the  $TE_1$  mode propagates in the unperturbed parallel plate waveguide. At millimeter-wave frequencies, the dependence of the characteristics of the periodically slotted parallel plate waveguide on the applied dc magnetic field is estimated numerically. It is theoretically explained how the characteristics can be tuned and the radiation patterns can be controlled by varying the dc magnetic field applied to the ferrite from the viewpoint of the leaky wave antenna application.

## 2. THEORETICAL ANALYSIS

Let us consider a periodically slotted parallel plate waveguide shown in Fig. 1 consisting of a finite periodic slot array formed in the upper plate of a parallel plate waveguide that is filled with ferrite magnetized in the  $z$  direction. In Fig. 1,  $b$ ,  $D$ ,  $L$  and  $2a$  show the height, the periodicity, the number of the slots and the slot width of the periodically slotted parallel plate waveguide, respectively. In Fig. 1, it is assumed that

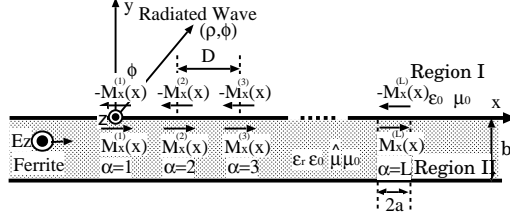


Fig. 2: Equivalent analytical model.

the electromagnetic field is uniform in the  $z$  direction (so that  $\frac{\partial}{\partial z} = 0$ ) and the time dependence is  $e^{j\omega t}$ . The relative permittivity of the ferrite is  $\epsilon_r$ . It is assumed that there is no loss in the ferrite used in the periodically slotted parallel plate waveguide. Then, the relative permeability tensor  $\hat{\mu}$  is given by

$$\hat{\mu} = \begin{bmatrix} \mu & j\kappa & 0 \\ -j\kappa & \mu & 0 \\ 0 & 0 & 1 \end{bmatrix}, \quad \mu = 1 + \frac{\omega_h \omega_m}{\omega_h^2 - \omega^2}, \quad \kappa = \frac{\omega \omega_m}{\omega_h^2 - \omega^2}, \quad (1)$$

$$\omega_h = \gamma \mu_0 H_0, \quad \omega_m = \gamma \mu_0 M_s.$$

where  $\mu_0$  is the free space permeability,  $\omega$  is the angular frequency,  $\mu_0 H_0$  is the applied dc magnetic field,  $\gamma$  is the gyromagnetic ratio ( $= 1.76 \times 10^{11} \text{ rad/T/sec}$ ) and  $\mu_0 M_s$  is the saturation magnetization of the ferrite. For the dielectric-filled slotted parallel plate waveguide in [22],[23], the cases in which both the permittivity and permeability are isotropic are analyzed. In the present paper, the case in which only the permeability is expressed with an anisotropic tensor is analyzed. In this paper, not only the magnetostatic mode obtained under the magnetostatic condition neglecting the electric field components, but also the electromagnetic modes containing the electric field components are rigorously analyzed.

Let us assume the case in which only the  $TE_1$  mode propagates in the parallel plate waveguide filled with ferrite as shown in Fig. 1. The slot regions  $S_\beta (\beta = 1, \dots, L)$  are defined as  $\{S_\beta : |x - (\beta - 1)D| \leq a, y = 0\}$  in Fig. 1. The analysis is carried out with the equivalent analytical model in Fig. 2, in which each slots is replaced with equivalent magnetic current  $M_x^{(\beta)}(x)$ . In this case, the incident electromagnetic field ( $E_{zI}^{inc}, H_{xI}^{inc}, H_{yI}^{inc}$ ), the scattered electromagnetic field in Region I ( $E_{zI}^s, H_{xI}^s, H_{yI}^s$ ), and the scattered electromagnetic field in Region II ( $E_{zII}^s, H_{xII}^s, H_{yII}^s$ ) are given as follows:

$$\begin{aligned} E_{zII}^{inc} &= \sin\left(\frac{\pi}{b}y\right)e^{-jk_{x1}x}, \\ H_{xII}^{inc} &= -\frac{1}{j\omega\mu_0\mu_{eff}} \left\{ \frac{\pi}{b} \cos\left(\frac{\pi}{b}y\right) + \frac{\kappa}{\mu} k_{x1} \sin\left(\frac{\pi}{b}y\right) \right\} e^{-jk_{x1}x}, \\ H_{yII}^{inc} &= -\frac{1}{\omega\mu_0\mu_{eff}} \left\{ k_{x1} \sin\left(\frac{\pi}{b}y\right) + \frac{\kappa}{\mu} \frac{\pi}{b} \cos\left(\frac{\pi}{b}y\right) \right\} e^{-jk_{x1}x}, \end{aligned} \quad (2)$$

$$\begin{aligned} E_{zI}^s &= \frac{j}{4} \sum_{\beta=1}^L \int_{S_\beta} M_x^{(\beta)}(x') \frac{\partial}{\partial y} \{ H_0^{(2)}(k_0 R^-) \\ &\quad + H_0^{(2)}(k_0 R^+) \} |_{y'=0+} dx', \\ H_{xI}^s &= \frac{1}{4k_0 Z_0} \sum_{\beta=1}^L \int_{S_\beta} M_x^{(\beta)}(x') (k_0^2 + \frac{\partial^2}{\partial x'^2}) \\ &\quad \{ H_0^{(2)}(k_0 R^-) + H_0^{(2)}(k_0 R^+) \} |_{y'=0+} dx', \\ H_{yI}^s &= \frac{1}{4k_0 Z_0} \sum_{\beta=1}^L \int_{S_\beta} M_x^{(\beta)}(x') \frac{\partial^2}{\partial x' \partial y} \\ &\quad \{ H_0^{(2)}(k_0 R^-) + H_0^{(2)}(k_0 R^+) \} |_{y'=0+} dx', \end{aligned} \quad (3)$$

$$R^\pm = \sqrt{(x - x')^2 + (y \mp y')^2}.$$

$$\begin{aligned} E_{zII}^s &= \sum_{\beta=1}^L \int_{S_\beta} M_x^{(\beta)}(x') G(x, y; x', y') |_{y'=0-} dx', \\ H_{xII}^s &= -\frac{1}{j\omega\mu_{eff}\mu_0} \sum_{\beta=1}^L \int_{S_\beta} M_x^{(\beta)}(x') \\ &\quad \cdot \left\{ \frac{\partial G(x, y; x', y')}{\partial y} \right. \\ &\quad \left. + j\frac{\kappa}{\mu} \frac{\partial G(x, y; x', y')}{\partial x} \right\} |_{y'=0-} dx', \\ H_{yII}^s &= \frac{1}{j\omega\mu_{eff}\mu_0} \sum_{\beta=1}^L \int_{S_\beta} M_x^{(\beta)}(x') \\ &\quad \cdot \left\{ \frac{\partial G(x, y; x', y')}{\partial x} \right. \\ &\quad \left. + j\frac{\kappa}{\mu} \frac{\partial G(x, y; x', y')}{\partial y} \right\} |_{y'=0-} dx', \end{aligned} \quad (4)$$

$$\begin{aligned} G(x, y; x', y') &= \frac{j}{b} \sum_{q=1}^{\infty} \frac{1}{k_{xq}} \left\{ q \frac{\pi}{b} \cos(q\pi \frac{y'}{b}) \right. \\ &\quad \left. + \frac{(x - x')}{|x - x'|} k_{xq} \frac{\kappa}{\mu} \sin(q\pi \frac{y'}{b}) \right\} \\ &\quad \cdot \sin(q\pi \frac{y}{b}) e^{-jk_{xq}|x - x'|}. \end{aligned} \quad (5)$$

$$\begin{aligned} k_{xq} &= \sqrt{\epsilon_r \mu_{eff} k_0^2 - (q\pi/b)^2}, \quad \mu_{eff} = \frac{\mu^2 - \kappa^2}{\mu}, \\ k_0 &= \omega \sqrt{\epsilon_0 \mu_0}, \quad Z_0 = \sqrt{\frac{\mu_0}{\epsilon_0}}. \end{aligned}$$

Here,  $\epsilon_0$  is the free space permittivity and  $H_0^{(2)}(\cdot)$  is zeroth-order Hankel function of the second kind. From the condition that the tangential components of the magnetic field in Region I and II are continuous over each slot region  $S_\beta$ , namely,

$$H_{xI}^s |_{y=0+} = H_{xII}^{inc} |_{y=0-} + H_{xII}^s |_{y=0-}, \quad \text{over } S_\beta (\beta = 1, 2, \dots, L) \quad (6)$$

the integral equation on the equivalent surface magnetic current  $M_x^{(\beta)}(x)$  over the  $\beta$ th slot can be obtained. All slot regions  $S_\beta$  are equally divided into  $N$  segments and each equivalent surface magnetic current  $M_x^{(\beta)}(x)$  is expanded in terms of the piecewise sinusoidal function  $\Phi_{n_\beta}^{(\beta)}(x)$  ( $n_\beta = 1, \dots, N - 1$ )

as

$$\begin{aligned}
M_x^{(\beta)}(x) &= \sum_{n_\beta=1}^{N-1} V_{n_\beta}^{(\beta)} \Phi_{n_\beta}^{(\beta)}(x) \\
V_{n_\beta}^{(\beta)} &: \text{unknown coefficients.} \\
\Phi_{n_\beta}^{(\beta)}(x) &= \frac{\Psi_{n_\beta}^{(\beta)}(x)}{\sin k_0 h} \\
\Psi_{n_\beta}^{(\beta)}(x) &= \sin k_0(x - x_{n_\beta-1}^{(\beta)})P_{n_\beta-1}^{(\beta)}(x) \\
&\quad + \sin k_0(x_{n_\beta+1}^{(\beta)} - x)P_{n_\beta}^{(\beta)}(x) \quad (7) \\
P_{n_\beta-1}^{(\beta)}(x) &= \begin{cases} 1 & x_{n_\beta-1}^{(\beta)} \leq x \leq x_{n_\beta}^{(\beta)} \\ 0 & \text{other} \end{cases} \\
x_{n_\beta-1}^{(\beta)} &= -a + (\beta - 1)D + (n_\beta - 1)h, \\
x_{n_\beta}^{(\beta)} &= -a + (\beta - 1)D + n_\beta h, \\
h &= \frac{2a}{N}.
\end{aligned}$$

When both sides of Eq. (6) are multiplied by  $\Psi_{m_\alpha}^{(\alpha)}(x) = \sin k_0 h \Phi_{m_\alpha}^{(\alpha)}(x)$  ( $m_\alpha = 1, 2, \dots, N-1, h = \frac{2a}{N}$ ) and are integrated over  $S_\alpha$  ( $\alpha = 1, 2, \dots, L$ ), then the above mentioned integral equation is reduced to the following equations as

$$[Y_{m_\alpha n_\beta}^{\alpha\beta}] [V_{n_\beta}^{(\beta)}] = [I_{m_\alpha}^{(\alpha)}] \quad (8)$$

$$Y_{m_\alpha n_\beta}^{\alpha\beta} = Y_{1m_\alpha n_\beta}^{\alpha\beta} + Y_{2m_\alpha n_\beta}^{\alpha\beta} \quad (9)$$

$$Y_{1m_\alpha n_\beta}^{\alpha\beta} = \frac{1}{j2 \sin k_0 h} k_0 S_{m_\alpha n_\beta}^{\alpha\beta} \quad (10)$$

$$k_0 S_{m_\alpha n_\beta}^{\alpha\beta} = 2 \cos k_0 h k_0 F_{m_\alpha n_\beta}^{\alpha\beta} - k_0 F_{m_\alpha n_\beta+1}^{\alpha\beta} - k_0 F_{m_\alpha n_\beta-1}^{\alpha\beta}$$

$$\begin{aligned}
k_0 F_{m_\alpha n_\beta}^{\alpha\beta} &= 2k_0 r_{m_\alpha n_\beta}^{\alpha\beta} H_1^{(2)}(k_0 r_{m_\alpha n_\beta}^{\alpha\beta}) \cos k_0 h \\
&\quad - k_0 r_{m_\alpha+1n_\beta}^{\alpha\beta} H_1^{(2)}(k_0 r_{m_\alpha+1n_\beta}^{\alpha\beta}) \\
&\quad - k_0 r_{m_\alpha-1n_\beta}^{\alpha\beta} H_1^{(2)}(k_0 r_{m_\alpha-1n_\beta}^{\alpha\beta}) \\
r_{m_\alpha n_\beta}^{\alpha\beta} &= |x_{m_\alpha}^{(\alpha)} - x_{n_\beta}^{(\beta)}|
\end{aligned}$$

$$\begin{aligned}
Y_{2m_\alpha n_\beta}^{\alpha\beta} &= \frac{1}{\mu_{eff} \sin k_0 h} [ \{ B_0 \delta_{m_\alpha n_\beta} \\
&\quad + B_1 (\delta_{m_\alpha n_\beta+1} + \delta_{m_\alpha n_\beta-1}) \} \delta_{\alpha\beta} \\
&\quad + \frac{k_0 b}{j\pi^2} \sum_{q=1}^{\infty} \frac{k_0}{k_{xq}} \frac{C_q^2}{q^2} T_{m_\alpha n_\beta}^{\alpha\beta}(q) ] \quad (11)
\end{aligned}$$

$$\begin{aligned}
B_0 &= -(k_0 b \sin 2k_0 h) U \\
&\quad - \frac{W}{2k_0 b} (2k_0 h - \sin 2k_0 h)
\end{aligned}$$

$$\begin{aligned}
B_1 &= (k_0 b \sin k_0 h) U \\
&\quad + \frac{W}{2k_0 b} (k_0 h \cos k_0 h - \sin k_0 h)
\end{aligned}$$

$$U = -\frac{\cot \sqrt{\varepsilon_r \mu_{eff} - 1} k_0 b}{2 \sqrt{\varepsilon_r \mu_{eff} - 1} k_0 b} + \frac{1}{2} \operatorname{cosec}^2 \sqrt{\varepsilon_r \mu_{eff} - 1} k_0 b$$

$$W = \sqrt{\varepsilon_r \mu_{eff} - 1} k_0 b \cot \sqrt{\varepsilon_r \mu_{eff} - 1} k_0 b$$

$$C_q = \frac{1}{1 - (\varepsilon_r \mu_{eff} - 1) \left( \frac{k_0 b}{q\pi} \right)^2}$$

$$T_{m_\alpha n_\beta}^{\alpha\beta}(q) = Q_{m_\alpha n_\beta+1}^{\alpha\beta}(q) + Q_{m_\alpha n_\beta-1}^{\alpha\beta}(q) - 2 \cos k_0 h Q_{m_\alpha n_\beta}^{\alpha\beta}(q)$$

$$\begin{aligned}
Q_{m_\alpha n_\beta}^{\alpha\beta}(q) &= e^{-jk_{xq} r_{m_\alpha+1n_\beta}^{\alpha\beta}} + e^{-jk_{xq} r_{m_\alpha-1n_\beta}^{\alpha\beta}} \\
&\quad - 2 \cos k_0 h e^{-jk_{xq} r_{m_\alpha n_\beta}^{\alpha\beta}}
\end{aligned}$$

$$I_{m_\alpha}^{(\alpha)} = \frac{2\pi k_0 e^{-jk_{x1} x_{m_\alpha}^{(\alpha)}}}{\mu_{eff} b (k_0^2 - k_{x1}^2)} (\cos k_{x1} h - \cos k_0 h). \quad (12)$$

In the above,  $H_1^{(2)}(\cdot)$  denotes the first-order Hankel function of the second kind. From the undetermined coefficients  $V_{n_\beta}^{(\beta)}$  obtained by solving the above mentioned matrix equation (8) and Eqs. (7), (3) and (4), the equivalent surface magnetic currents and the scattered electromagnetic fields at each region can be determined.

The far field expression for the electric field  $E_{zI}(\rho, \phi)$  due to the equivalent magnetic current source is

$$\begin{aligned}
E_{zI}(\rho, \phi) &= \sqrt{\frac{2}{\pi k_0 \rho}} e^{-j(k_0 \rho - \frac{\pi}{4})} \\
&\quad \cdot \frac{\{ \cos(k_0 \sin \phi h) - \cos k_0 h \}}{\sin k_0 h \cos \phi} \quad (13) \\
&\quad \cdot \sum_{\beta=1}^L \sum_{n_\beta=1}^{N-1} V_{n_\beta}^{(\beta)} e^{jk_0 \sin \phi x_{n_\beta}^{(\beta)}}
\end{aligned}$$

The incident power per unit length in the z direction in this parallel plate waveguide  $P_{inc}$ , the Poynting power in the  $\rho$  direction  $p_s(\rho, \phi)$ , the radiated power  $P_{rad}$  and the radiation efficiency  $\eta_{rad}$  are given by

$$P_{inc} = -\frac{1}{2} \operatorname{Re} \{ \int_{-b}^0 E_{zII}^{inc} H_{yII}^{*inc} dy \} \quad (14)$$

$$p_s(\rho, \phi) = \frac{1}{2} \operatorname{Re} \{ E_{zI}(\rho, \phi) H_{\phi I}^*(\rho, \phi) \}, \quad (15)$$

$$P_{rad} = \int_{-\frac{\pi}{2}}^{\frac{\pi}{2}} p_s(\rho, \phi) \rho d\phi, \quad (16)$$

$$\eta_{rad} = \frac{P_{rad}}{P_{inc}}. \quad (17)$$

The radiation pattern is defined as

$$G_{rad}(\phi) = 10 \log_{10} \{ 2\pi \rho \frac{p_s(\rho, \phi)}{P_{inc}} \}. \quad (18)$$

### 3. NUMERICAL RESULT

In the numerical calculations, the relative permittivity  $\varepsilon_r$  and saturation magnetization  $\mu_0 M_s$  of the ferrite and the number of the slots  $L$ , the slot width  $2a$ , the periodicity  $D$  and height  $b$  of the periodically slotted parallel plate waveguide filled with ferrite are

$$\varepsilon_r = 12.5 \quad \mu_0 M_s = 0.5T [25] - [27].$$

$$L = 60 \quad 2a = 1.0mm \quad D = 3.0mm \quad b = 1.5mm.$$

In the numerical calculation, ferrite is assumed to be lossless. The number of divisions of the slot region  $N$  is fixed to  $N = 40$  so that the width of the divided slot region  $h$  can be smaller than  $\frac{1}{50}$  of the wavelength. The order of the truncated terms  $N_{tr}$  in the infinite series in Eq. (5) is fixed to  $N_{tr} = 200$ .

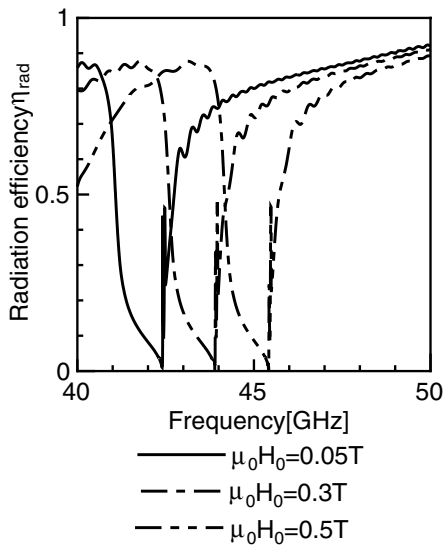


**Fig. 3:** The Frequency dependent characteristic of the radiation efficiency  $\eta_{rad}$  of the finite periodic slot array in the parallel plate waveguide filled with the transversely magnetized ferrite.

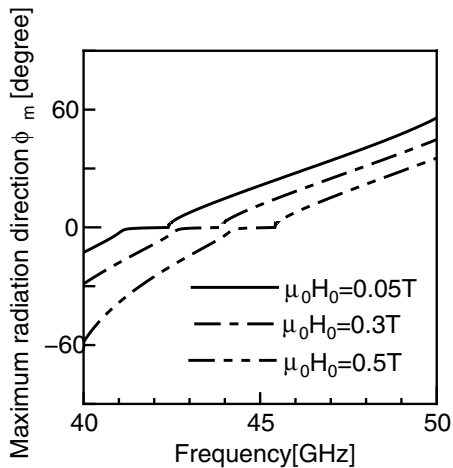


**Fig. 4:** The Frequency dependent characteristic of the maximum radiation direction  $\phi_m$  of the finite periodic slot array in the parallel plate waveguide filled with the transversely magnetized ferrite.

Also, it is confirmed that the numerical results satisfy the energy conservation law within an error of  $10^{-3}\%$ .

Fig. 3 shows the frequency dependent characteristic of the radiation efficiency  $\eta_{rad}$  at 40 to 50GHz for different values of the applied dc magnetic field. In the case of  $\mu_0 H_0 = 0.05T$ , the maximum radiation efficiency is about 0.9, and the frequency band for a radiation efficiency of less than 0.1 is caused by the Bragg reflection near 42GHz. If the applied dc magnetic field is changed from  $\mu_0 H_0 = 0.05T$  to  $\mu_0 H_0 = 0.5T$ , it is found that the radiation range is tuned by about 3GHz, while the maximum radiation efficiency and the radiation bandwidth do not essentially change. From

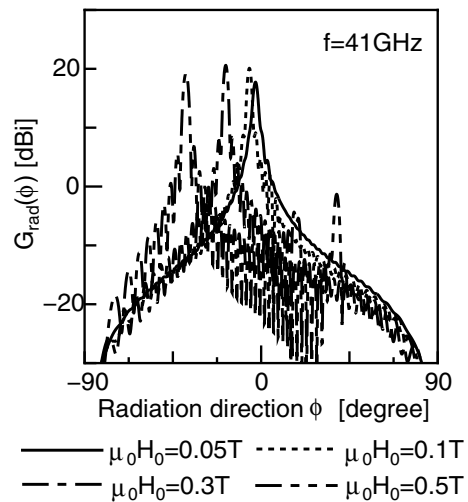


**Fig. 5:** The radiation pattern  $G_{rad}(\phi)$  of the finite periodic slot array in the parallel plate waveguide filled with the transversely magnetized ferrite at 41GHz.

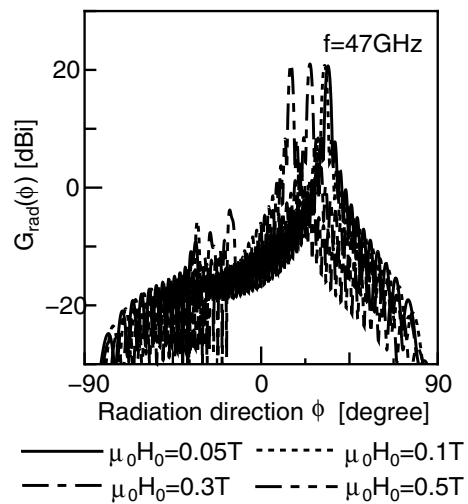


**Fig. 6:** The radiation pattern  $G_{rad}(\phi)$  of the finite periodic slot array in the parallel plate waveguide filled with the transversely magnetized ferrite at 47GHz.

the above results, it is found that the operating frequency can be varied by simply changing the applied dc magnetic field without changing the physical dimensions. Therefore, there is possibility of constructing antenna suitable for various millimeter-wave systems.

Fig. 4 shows the frequency characteristics of the maximum beam direction  $\phi_m$  of the radiated wave in the range of 40 to 50GHz, dependent on the applied dc magnetic field. From Fig. 4 it is found that the maximum beam direction  $\phi_m$  show the marked frequency beam-scanning characteristics. Specially, in the case of  $\mu_0 H_0 = 0.05T$ , the maximum beam direction  $\phi_m$  changes from  $-12.8^\circ$  to  $55.8^\circ$  in the range of 40 to 50GHz and

the Bragg reflection band with the bandwidth of about 1GHz is caused in the range of 41 to 43GHz. Also, if the applied dc magnetic field is varied from  $\mu_0 H_0 = 0.05T$  to  $\mu_0 H_0 = 0.5T$ , the frequency dependence of the maximum beam direction  $\phi_m$  is tuned by about 3GHz.

Figs. 5 and 6 show the dependence of the radiation pattern  $G_{rad}(\phi)$  on the applied dc magnetic field at 41GHz and the dependence of the the radiation pattern  $G_{rad}(\phi)$  on the applied dc magnetic field at 47GHz. In the case of  $\mu_0 H_0 = 0.05T$ , The maximum beam directions  $\phi_m$  of Fig. 5 and Fig. 6 are  $-2.92^\circ$  and  $32.1^\circ$ , respectively. From this, too, it is found that the maximum beam direction  $\phi_m$  shows the marked frequency beam-scanning characteristic. Also, as the applied dc magnetic field  $\mu_0 H_0$  is varied from 0.05T to 0.5T, the maximum beam direction  $\phi_m$  is scanned from  $-2.92^\circ$  to  $-38.3^\circ$  in Fig. 5 and from  $32.1^\circ$  to  $15.1^\circ$  in Fig. 6. Further, it is found that the intensity of the radiated power is changed with the beam scan by the applied dc magnetic field, because the beam scan is caused with the tune of the radiation frequency band by the applied dc magnetic field.

#### 4. CONCLUSION

Radiation characteristics of a finite periodic slot array in a upper plate of a parallel plate waveguide filled with a transversely magnetized ferrite is analyzed by the method of moments in the case which only the  $TE_1$  mode propagates in the unperturbed parallel plate waveguide. Under the assumption that ferrite loss is nonexistent, it is theoretically explained how the frequency dependent characteristic of the radiation efficiency and the frequency scanning characteristic of the radiated wave are controlled by varying the applied dc magnetic field. From numerical results, it is found that the frequency dependent characteristic of the radiation efficiency  $\eta_{rad}$  and the frequency dependent characteristic of the maximum beam direction  $\phi_m$  are tuned to higher frequency band without significantly changing the maximum radiation efficiency and the radiation frequency bandwidth by varying the applied dc magnetic field. Also, it is explained that the beam scanning of the radiation patterns are caused with the tuning of the frequency dependence of the maximum beam direction by changing the applied dc magnetic field.

#### REFERENCES

- [1] Special Session on Microwave Analog Smart Devices and Circuits, IEICE Trans. C, vol. J87-C, no. 1, Jan. 2004.
- [2] "SPECIAL SECTION ON MICROWAVE MAGNETICS," Proc. IEEE, vol. 76, no. 2, Feb. 1988.
- [3] Y. Konishi, Recent advances in microwave circuit techniques with ferrite. IEICE 1972.
- [4] T. Hashimoto, Microwave ferrite and its application. Sogo-Denshi Publication 1997.
- [5] D. J. Angelakos, M. M. Korman, "Radiation from ferrite-filled apertures," Proc. IRE, vol. 44, pp. 1463-1468, 1956.
- [6] G. Tyras and G. Held, "Radiation from a rectangular waveguide filled with ferrite," IRE Trans. Microwave Theory & Tech., vol. MTT-6, pp. 268-277, July 1958.
- [7] N. Okamoto and S. Ikeda, "An experimental study of electronic scanning by an antenna loaded with a circular array of ferrite rods," IEEE Trans. Antenna Propag., vol. AP-27, no. 3, pp. 426-429, May 1979.
- [8] K. Araki and T. Itoh, "Analysis of periodic ferrite slab waveguides by means of improved perturbation method," IEEE Trans. Microwave Theory & Tech., vol. MTT-29, no.9, pp. 911-916, Sept. 1981.
- [9] T. Ohira, M. Tsutsumi, and N. Kumagai, "Radiation of millimeter waves from a grooved ferrite image line," Proc. IEEE, vol. 70, pp.682-683, June 1982.
- [10] . Maheri, M. Tsutsumi, and N. Kumagai, "Experimental studies of magnetically scannable leaky-wave antennas having a corrugated ferrite slab/dielectric structure," IEEE Trans. Antenna & Propagat., vol. 36, no. 7, pp. 911-917, July 1988.
- [11] S. Erkin, N. S. Chang, H. Maheri, and M. Tsutsumi, "Characteristics of millimeter wave radiation in a corrugated ferrite slab structure," IEEE Trans. Microwave Theory & Tech., vol. MTT-36, no.3, pp.568-575, March 1988.
- [12] A. Henderson, J. R. James, and D. Fray, "Magnetised microstrip antenna with pattern control," Electron. Lett., vol. 24, pp. 45-47, Jan. 1988.
- [13] D. Pozar and V. Sanchez, "Magnetic tuning of a microstrip antenna on a ferrite substrate," Electron. Lett., vol. 24, pp. 729-731, June 1988.
- [14] D. Pozar, "Radiation and scattering characteristics of microstrip antennas on normally biased ferrite substrates," IEEE Trans. Antennas Propagat., vol. 40, no.9, pp.1084-1092, Sept. 1992.
- [15] P. J. Rainville and F. J. Harackiewicz, "Magnetic turning of a microstrip patch antenna fabricated on a ferrite film," IEEE Microwave Guided Wave Lett., vol. 2, no. 12, Dec. 1992.
- [16] N. E. Buris, T. B. Funk, and R. S. Silvertine, "Dipole arrays printed on ferrite substrates," IEEE Trans. Antennas Propagat., vol. 41, no.2, pp.165-175, Feb. 1993.
- [17] H.-Y. Yang, J. A. Castaneda, and N. G. Alexopoulos, "The RCS of a microstrip patch on an arbitrarily biased ferrite substrate," IEEE Trans. Antenna Propagat., vol. 41, pp. 1610-1614, Dec. 1993.
- [18] B. Lee, and Frances J. Harackiewicz, "The RCS of a microstrip antenna on in-plane biased ferrite substrate," IEEE Trans. Antenna Propagat., vol. 44, pp. 208-211, Feb. 1996.
- [19] C. Surawatpunya, M. Tsutsumi, and N. Kumagai, "Bragg interaction of electromagnetic waves in a ferrite slab periodically loaded with metal strips," IEEE Trans. Microwave Theory & Tech., vol. MTT-32, no. 7, pp. 689-695, July 1984.
- [20] M. Ozaki, M. Asai, J. Yamakita, S. Sawa, "Analysis of ferrite slab waveguides with resistive planar grating," IEICE Trans. C-I, vol. J75-C-I, no. 11, pp. 694-702, Nov. 1992.
- [21] K. Nishimura, "Radiation Characteristics of a Slotted Parallel Plate Waveguide Filled with a Transversely Magnetized Ferrite," IEICE Trans. C, vol. J84-C, no. 11, pp. 1061-1067, Nov. 2001.
- [22] C. W. Chuang, "Generalized admittance matrix for a slotted parallel-plate waveguide," IEEE Trans. Antennas Propagat., vol. 36, no. 9, pp.1227-1230, Sept. 1988.
- [23] J.-I. Lee, U.-H. Cho and Y.-K. Cho, "Analysis of a dielectrically filled parallel-plate waveguide with finite number of periodic slots in its upper wall as a leaky-wave antenna," IEEE Trans. Antennas Propagat., vol. 47, no. 4, pp. 701-706, Sept. 1988.
- [24] K. Nishimura, "Radiation Characteristics of a Finite Periodic Slot Array in a Parallel Plate Waveguide Filled with a Transversely Magnetized Ferrite," Tech. Rep. IEICE Japan, MW-04-06, June 2004.
- [25] M. Geshiro and T. Itoh, "Analysis of double-layer finelines containing a magnetized ferrite," IEEE Trans. Microwave Theory & Tech., vol. MTT-35, no. 12, pp. 1377-1381, Dec. 1987.
- [26] T. Kitazawa, "Analysis of shielded striplines and finlines with finite metallization thickness containing magnetized ferrite," IEEE Trans. Microwave Theory & Tech., vol. MTT-39, no. 1, pp. 70-74, Jan. 1991.
- [27] K. Hirayama, S. Takimoto, Y. Hayashi, M. Koshiba, "Finite element analysis of finelines with magnetized lossy ferrite," IEICE Trans. C-I, vol. J80-C-I, no. 3, pp. 109-118, March 1997.
- [28] Mini-Special Issue on Millimeter-Wave Technology and its Applications. IEICE Trans. vol. J77-C-I, no. 11, Nov. 1994.
- [29] T. Teshirogi and T. Yoneyama, Wave-Summit Series. New millimeter-wave technology. Ohm Press; 1999.